1987

Electrical Testing of Piezoelectric Transducers Applied to Accelerometer Design

Patrick L. Heron
University of Central Florida

ELECTRICAL TESTING OF PIEZOELECTRIC TRANSDUCERS APPLIED TO ACCELEROMETER DESIGN

BY

PATRICK L. HERON
B.S.E., California State University, Sacramento, 1983

THESIS

Submitted in partial fulfillment of the requirements
for the degree of Master of Science in Engineering
in the Graduate Studies Program of the College of Engineering
University of Central Florida
Orlando, Florida

Summer Term
1987

ABSTRACT

Piezoelectric transducers are, by nature, electromechanical devices. Methods historically used to characterize these transducers involve both electrical and mechanical measurements.

The purpose of this paper is to propose a technique to characterize piezoids which will require electrical measurements only. Thus, characterization can be accomplished through the use of readily available calibrated electrical test equipment. This technique is based upon the assumption that some insight into the dynamic behavior of a piezoid can be implied by inspection of the transducer's static material properties. A necessary condition for the validity of the proposed technique is established. This test procedure is utilized in the design/test process of a piezoelectric accelerometer.

TABLE OF CONTENTS

LIST OF TABLES iv

LIST OF FIGURES v

LIST OF SYMBOLS vi

INTRODUCTION 1

Chapter

I. STATIC DESCRIPTION OF CERAMIC TRANSDUCERS 5

II. STATIC DESCRIPTION OF QUARTZ TRANSDUCERS 13

III. TRANSDUCER DYNAMIC MODEL 19

IV. ELECTRICAL TESTING 23

V. ELECTROMETER DESIGN 30

VI. MECHANICAL TESTING 35

VII. RESULTS 39

VIII. CONCLUSION 42

Appendices

A. PHYSICAL PROPERTIES OF SELECTED MATERIALS 45

B. ROTATION MATRICES 46

REFERENCES 51

LIST OF TABLES

1. Static Capacitance and Induced Potential Per Pascal Stress for a Cylindrical Disk with r = 1.5 cm and t = 5 mm 11

2. Ratio of Mechanically Induced to Electrically Induced Strain for a BT-Cut Quartz Plate 29

3. Electroelastic Coefficients for Quartz 50

4. Electroelastic Coefficients for the Lead-Zirconate-Titanate Ceramic PZT-5 50

LIST OF FIGURES

1. A Typical Piezoelectric Accelerometer Showing All Components of Stress Applied to the Transducer During General Acceleration 4

2. Progressive Rotation of Axes for a BT-Cut Quartz Plate . . 16

3. Model of a Piezoelectric Transducer Near One of its Resonant Vibrational Modes 20

4. Transducer Model used in Analysis 22

5. Op-amp Model used for Circuit Analysis 31

6. Amplifier Configuration 33

7. Acceleration Profile used to Determine Accelerometer Impulse Response 36

LIST OF SYMBOLS

Symbol	Definition
$\underline{c}$	Stiffness
$\underline{x}$	Strain
$\underline{D}$	Electric displacement
$\underline{k}$	Dielectric Constant
$\underline{s}$	Compliance
$\underline{X}$	Stress
$\underline{E}$	Electric Field
$\underline{d}$	Piezoelectric stress coefficient
$\underline{e}$	Piezoelectric strain coefficient
$\underline{q}$	Piezoelectric voltage coefficient
$\underline{t}$, $\underline{u}$, $\underline{v}$	3 x 3 rotation matrix about x-, y-, z-axis
$\underline{T}$, $\underline{U}$, $\underline{V}$	6 x 6 rotation matrix about x-, y-, z-axis
p	Angle of rotation about x-axis
q	Angle of rotation about y-axis
r	Angle of rotation about z-axis
c_e	Electrostatic capacitance

INTRODUCTION

It is well known that piezoelectric materials develop electric displacement that is proportional to mechanical strain. Conversely, application of an electric field will produce mechanical strain in a piezoelectric material. These properties, dubbed the forward and inverse piezoelectric effects, are the basis for numerous commercial devices. The forward effect has been used to measure mechanical force or pressure in applications such as sonar transducers (6) and accelerometers (10). The inverse effect has been used in applications including acoustic transduces and micro positioners (2). (It is interesting to note that, due to anisotropy, reciprocity between the forward and inverse effects does not necessarily exist.)

Piezoelectric materials are useful because they form a bridge between the mechanical and the electrical domain. Methods used to characterize piezoids understandably measure both mechanical and electrical properties of the transducer. Two schemes are commonly used to measure mechanical properties.

In the first method, a transducer is subjected to a known mechanical input while the electrical response is recorded. For example an accelerometer under test is placed on a shake-table along with a calibrated accelerometer. The electrical response of the device under test is compared with the response of the calibrated

accelerometer (10). In the second method, a transducer is driven electrically and the mechanical response is measured. For instance, the acoustic power output of a transducer can be measured with a calibrated microphone as the frequency of the electrical input is swept throughout a desired range.

Measurement of mechanical properties requires equipment that is uncommon to the test bench of the electrical engineer. Additionally, this equipment is difficult to calibrate; electrical standards are more easily produced than are mechanical standards. It is desirable to be able to characterize a piezoelectric transducer using electrical measurements only. Thus, calibrated electrical test equipment can be used.

A test procedure is proposed to characterize transducers based solely upon electrical measurements. A limited form or reciprocity is necessary for the test to be valid. It is assumed that the existence of this limited reciprocity for transducers under dynamic conditions can be predicted by studying the static properties of the material. If the validity of electrical testing is established for a single material, the test will also be valid for materials having the same internal crystal symmetry. The testability of all piezoelectric materials in each of the twenty crystalline classes can easily be determined.

This paper will focus largely upon the study of piezoelectric accelerometers. Properties pertinent to design of accelerometers will be examined. The purpose of this very specific approach is

twofold. First, the study of this specific application will provide a vehicle to introduce the notation and symbology that will be used throughout this paper. Second, the study of accelerometers will establish the need for device testing and will provide a concrete example of application of the test procedure on a practical device. Methods used here to test piezoelectric accelerometers can be tailored to characterize other piezoelectric devices. Accelerometers will now be discussed to illuminate the material properties of significance for this application.

One of the simplest and most rugged accelerometers is the bulk transducer type piezoelectric accelerometer. Figure 1 illustrates typical construction of such a device. The devices are comprised of a piezoelectric element which commonly consists of either a piezoelectric crystal such as quartz, or a ferroelectric ceramic. The element has conductive electrodes deposited on opposite faces. The transducer is sandwiched between a base and a seismic mass. As the transducer is accelerated, the mass, being bonded to the transducer, is forced to follow the acceleration of the transducer. The seismic mass exerts either a shear or normal reaction force on the transducer. The resulting transducer strain produces polarization which is detected by electronics. This type of device is classified as an unbalanced mass, bulk piezoelectric accelerometer.

It is desired that the device exhibit a high degree of immunity to components of acceleration orthogonal to the direction of the

acceleration being measured. This permits determination of acceleration in three dimensions by use of three accelerometers and simple vector operations (i.e., no compensation is needed for off-axis components of acceleration).

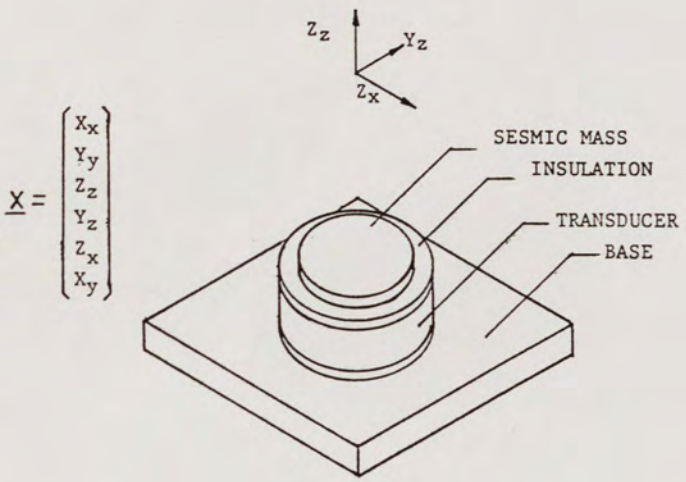

Figure 1. A Typical Piezoelectric Accelerometer Showing All Components of Stress Applied to the Transducer During General Acceleration.

It will be shown later that D.C. accelerations cannot be detected by an unbalanced accelerometer. This is a result of the small electrical capacitance of the transducer and finite input impedance of the amplifier. The electrical output of the accelerometer will roll off for low frequency acceleration. It is desirable to be able to measure low frequency vibrations. The design goal will be to have a half power output signal for vibrations at or below 0.10 Hz.

CHAPTER I

STATIC DESCRIPTION OF CERAMIC TRANSDUCERS

A fundamental understanding of the electromechanical properties of materials can be gained by considering the response of a transducer to constant or D.C. acceleration. This D.C. treatment will allow introduction of nomenclature and pertinent equations which will later be used in quasi-static or steady state A.C. analysis. This fundamental understanding is needed for formulation of a transducer test procedure. A major emphasis of this design is to extend accelerometer response to the lowest possible acceleration frequency. The study of accelerometer transient response to D.C. acceleration will permit selection of suitable materials to meet design goals and will also set criteria for electrometer design. An estimation of accelerometer output will be performed to permit selection of a suitable seismic mass. Transducer geometry will be assumed to be a thin cylindrical disk.

The following two equations are used in modeling a linear (but not necessarily isotropic) piezoelectric material (4).

$$\underline{D} = \underline{kE} + \underline{dX} \qquad [1.1]$$

$$\underline{x} = \underline{sX} + \underline{dE} \qquad [1.2]$$

The first term on the right of equation [1.1] indicates the relationship between an external electric field and the resultant electric displacement (as is the case for all dielectrics). The second terms indicate that additional polarization will be caused by application of mechanical stress. This relationship is a statement of piezoelectric effect.

Equation [1.2] indicates that mechanical strain in a piezoelectric material can be caused by application of mechanical stress and also by application of an external electric field. This second phenomenon is the inverse piezoelectric effect. Note that these are not scalar equations.

It can be shown that for an object in equilibrium, any mechanical stress or strain on the object can be resolved into three orthogonal normal stresses/strains and three orthogonal shear stresses/strains (1). Therefore, $\underline{x}$ and $\underline{X}$ are six vectors. In general piezoelectric materials are anisotropic; in fact, absence of a center of symmetry of crystalline structure is a pre-requisite for piezoelectricity (2). Material properties of piezoelectric substances are therefore dependant upon direction and cannot be represented by scalars. Compliance, $\underline{s}$, and stiffness, $\underline{c}$, are represented by 6 x 6 matrices to account for all possibilities relating terms of the stress and strain six vectors. Similarly, $\underline{d}$ and $\underline{e}$ are represented by 3 x 6 matrices and $\underline{k}$ by a 3 x 3. Piezoelectric materials do show symmetry about planes; a consequence of this symmetry is that some terms of the coefficient matrices are

zero. Conservation of mechanical and electrostatic energy results in terms of the matrices being dependant (4). Similar crystal structure results in the same general form for coefficient matrices. Thus, conclusions made regarding the behavior of a specific material are also valid for all piezoelectrics sharing the same crystalline structure. Reference (3) specifies the general form of the coefficient matrices for many classes of piezoelectric material. Those applicable to this work are reproduced in Appendix A.

It is often necessary to determine the effect that pure mechanical or pure electrical excitation has on a piezoid; under these constraints equations [1.1] and [1.2] can be decomposed.

$$\underline{D} = \underline{dX} \qquad [1.1a]$$

$$\underline{D} = \underline{kE} \qquad [1.1b]$$

$$\underline{x} = \underline{sX} \qquad [1.2a]$$

$$\underline{x} = \underline{dE} \qquad [1.2b]$$

These relationships can be combined to yield:

$$\underline{X} = \underline{eE} \qquad [1.3]$$

Where the piezoelectric strain coefficient, $\underline{e}$, is related to the compliance and the stress coefficient by the relationship $\underline{es} = \underline{d}$.

To get an approximation of the voltage output from a transducer per pascal applied pressure, consider a cylindrical disk piezoid of

thickness t and radius r oriented axially along the z-axis of a cartesian coordinate system (it is assumed that the piezoid is poled normally to its faces). A seismic mass is placed on the positive z-face of the piezoid. Upon acceleration the material may be subjected to combinations of normal stress along the z-axis (Z_z) as well as shear stress on the z-face along the x-axis (X_z) and along the y-axis (Y_z). (Due to the requirement of static equilibrium, $Z_x = X_z$). No other stresses are possible. We need to determine the induced potential difference between electrodes placed on the positive and negative z-faces as a function of normal stress along the z-axis.

Equation [1.3] can be rewritten as $\underline{E} = \underline{e}^{-1}\underline{X}$ and then solved for E_z. The potential across the plates is $v_z = E_z t$. Unfortunately, values for $\underline{e}$ are not published, while the values of $\underline{k}$ and $\underline{d}$ are. The result may be achieved by rewriting equation [1.1b] as $\underline{E} = \underline{k}^{-1}\underline{D}$ and combining with equation [1.1a] to give:

$$\underline{E} = \underline{k}^{-1}\underline{d}\underline{X} \qquad [1.4]$$

PZT and PLZT are commercially used piezoelectric ceramics. They have hexagonal crystalline structure of class C_{6v} and have piezoelectric stress coefficient and dielectric constant matrices, as indicated in Appendix A.

Substituting into equation [1.4], we arrive at the following result:

$$E_x = \frac{Z_x d_{15}}{k_{11}}$$

$$E_y = \frac{Y_z d_{15}}{k_{11}}$$

$$E_z = \frac{X_x d_{13}}{k_{33}} + \frac{Y_y d_{31}}{k_{33}} + \frac{Z_z d_{33}}{k_{33}} \qquad [1.5]$$

Of the three resulting equations, the third is applicable to the situation under consideration. Notice that the shear stresses that will be present in the design will not contribute to electric field along the z-axis. Thus this transducer will be able to measure acceleration along the z-axis and will be immune to interference from acceleration along any other axis.

For the stresses that will be present, equation [1.5] reduces to the following:

$$E_z = \frac{Z_z d_{33}}{k_{33}} \qquad [1.5a]$$

which permits easy calculation of the acceleration induced electric field. To determine the potential between the electrodes assume constant electric field with no fringing. The potential difference

is just the electric field strength times the thickness of the piezoid.

$$v = \frac{Z_z t d_{33}}{k_{33}} \qquad [1.6]$$

As will be seen later, magnitude of induced voltage is a minor consideration in this design. Voltage can always be boosted by additional gain in the electrometer. More important is the amount of actual electric displacement induced. For a given electrometer input resistance, the accelerometer will be able to respond to lower frequency vibrations if it has larger electric displacement. If the device is subjected to D.C. acceleration, the induced electric displacement will be "covered up" as charge leaks onto the electrodes through the finite input resistance of the electrometer. The output will remain unaffected longer if, for the same induced potential, there can be an increase in electric displacement. In other words, we desire that the device have as large as possible a static capacitance. This requires a large dielectric constant along the axis normal to the face of the transducer.

Neglecting electric field fringing, we can estimate capacitance using the equation for a parallel plate capacitor.

$$C_e = \frac{k_{33} \pi r^2}{t} \qquad [1.7]$$

Table 1 lists the electrostatic potential induced per pascal of applied stress and static capacitance for transducers having r = 1.5 cm and t = 5 mm. Table 1 permits comparison of the relative merits of several representative piezoelectric materials and also provides insight into the electrical characteristics of the transducer at a circuit level.

TABLE 1

STATIC CAPACITANCE AND INDUCED POTENTIAL PER PASCAL STRESS FOR A CYLINDRICAL DISK WITH r = 1.5 cm AND t = 5 mm

MATERIAL	C_e (nF)	μv/Pa
La/Zr/Ti		
2/65/35	0.815	130.
8/65/35	4.25	115.
7/60/90	4.50	111.
$BaTiO_2$	2.10	63.
Lead Zirconate Titonate (PZT-5)	2.10	124.
Lithium Sulfate	0.012	875.
Lead Meta Niobate	0.280	212.
X-cut Quartz	0.0056	290.

Using the information of Table 1, it is easy to calculate the thickness of steel needed for a seismic mass to provide a desired voltage output. For example, if an output of 1 mV/G is desired and

the transducer can supply 90 μv/Pa, the thickness of steel needed is calculated using equation [1.8] to be 0.143 mm.

$$T = \frac{k_{33} v}{t g_{33} PG} \qquad [1.8]$$

Note that the mass of the piezoid itself will cause the voltage output to be greater than predicted by [1.8]. At first glance it seems that very high output voltages may be attained by selecting a large seismic mass. This is undesirable as it may cause the device to act nonlinearly and, as will be seen later, will degrade the accelerometer's high frequency response.

CHAPTER II

STATIC DESCRIPTION OF QUARTZ TRANSDUCERS

Piezoelectric ceramics all have coefficient arrays of the same form as the hexagonal crystal class C6v; quartz has triagonal symmetry and is of the class D3 (3). Quartz was chosen for study because it has properties that are different than the ceramics and also because quartz is readily available. It is customary, when referring to quartz, to position the crystal so that the Z-axis of a cartesian coordinate system aligns with the optical axis of the crystal, and the X-axis aligns with the crystal's electrical axis (4). This convention will be used.

Let us first consider an X-cut quartz plate. The plate is cut from a crystal with it's faces normal to the electrical axis (X-axis). From Table 1 we can see that the plate will produce a fairly large potential but will have quite a small capacitance due to a small dielectric constant. Using equation [1.4] and the appropriate coefficient arrays from Appendix A, we can see that an X-cut plate is suitable for accelerometer work. The result of this calculation, equation [2.1], shows that a potential difference between the X-faces can be produced by normal stress along the Y-axis, normal stress along the X-axis, shear stress along the Y-axis applied to the Z-face. Of these, only normal stress along the X-axis can be produced by a seismic mass bonded to the X-face.

The X-cut plate will be immune to interference due to off-axis acceleration.

$$E_x = \frac{X_x d_{11}}{k_{11}} - \frac{Y_y d_{11}}{k_{11}} + \frac{Y_z d_{14}}{k_{11}}$$

$$E_y = -\frac{Z_x d_{14}}{k_{11}} - \frac{ZX_y d_{11}}{k_{11}}$$

$$E_z = 0 \qquad [2.1]$$

Quartz crystal plates designed for use as resonators are easy to obtain; however, in general, the plates are not cut with faces normal to any of the coordinate axes. (Quartz blanks cut this way are called rotated cuts.) For this reason, an X-cut plate could not be obtained. Rotated cuts make analysis complicated: to perform calculations stresses need to be expressed in terms of components which are parallel to the axes of the coordinate system. Applied stresses can easily be resolved into components which are normal to the faces of the plate. Unfortunately, the faces are not aligned with the coordinate axes (these are set by the physical properties of the material) so the applied stresses are difficult to represent. One method used to overcome this difficulty is to rotate the coordinate system to align the coordinate axes with the faces of the

quartz plate. In the new coordinate system stresses are easily represented in terms of component stresses which align with the new axes. The act of rotating the axes transforms the coefficient arrays generating new coefficient arrays which are valid in the new coordinate system. Appendix B gives the rotation matrices needed to rotate about any of the three coordinate axes. General rotations are performed by sequentially rotating about one axis at a time.

Figure 2a shows the orientation of a BT-cut plate with respect to the crystal coordinate axes. To facilitate, analysis two rotations will be performed to align the plate with the coordinate axes. The coordinate system will first be rotated 60^{o} about the Z-axis leaving the plate aligned as depicted in Figure 2b. The rotation is accomplished through use of the 3 x 3 rotation matrix $\underline{v}$ which rotates 3-vectors about the Z-axis, and $\underline{V}$ a 6 x 6 rotation matrix which rotates stress vectors about the Z-axis. Both rotation matrices are evaluated at 60^{o}. Equation [1.4] is pre-multiplied by $\underline{v}$.

$$\underline{vE} = \underline{vk}^{-1}\underline{dX}$$

The first term can be thought of as the electric field in the new coordinate system, this will be represented as $\underline{E}'$. We need to transform the stress vector to this new coordinate system. The stress vector will be pre-multiplied by the identity matrix in the following form:

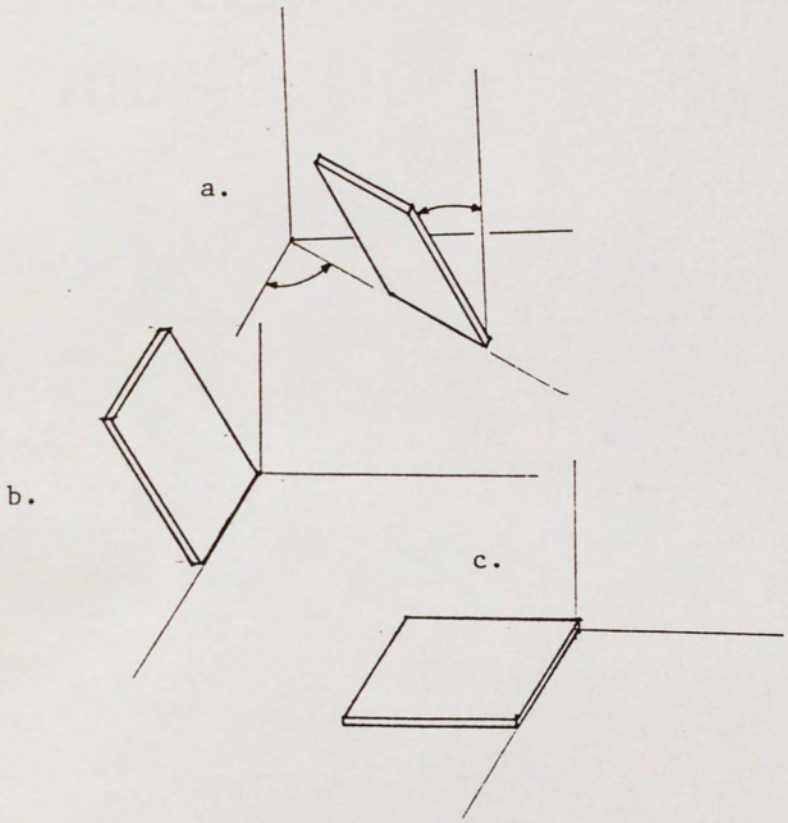

Figure 2. Progressive Rotation of Axes for a BT-Cut Quartz Plate.

$$\underline{I} = \underline{V}^{-1}\underline{V}$$

This results in

$$\underline{vE} = \underline{vk}^{-1}\underline{dV}^{-1}\underline{VX}$$

which may be written more compactly as:

$$\underline{E}' = \underline{vk}^{-1}\underline{dV}^{-1}\underline{X}'$$

The same procedure is utilized to rotate the coordinate system about the X-axis. This rotation will result in the orientation depicted in Figure 2c. If we let

$$\underline{E}'' = \underline{tE}' \quad \text{and} \quad \underline{X}'' = \underline{TX}'$$

where the rotation matrices $\underline{t}$ and $\underline{T}$ are evaluated at -41^{o}, then the result is equation [2.2].

$$\underline{E}'' = \underline{g}''\underline{X}'' \qquad [2.2a]$$

$$\underline{g}'' = \underline{tvk}^{-1}\underline{dV}^{-1}\underline{T}^{-1} \qquad [2.2b]$$

Algebraic solution of equation [2.2b] would prove quite tedious; results were calculated using the numerical values for quartz from

Appendix A. The result appears as equation [2.3] (units are mV M/Nt).

$$g'' = \begin{pmatrix} -0.0569 & 0.0 & 0.0 \\ 0.407 & 0.0 & 0.0 \\ 0.0162 & 0.0 & 0.0 \\ 0.0540 & 0.0 & 0.0 \\ 0.0 & 0.0658 & 0.0573 \\ 0.0 & 0.0565 & 0.0491 \end{pmatrix} \qquad [2.3]$$

Equation [2.3] is now substituted into equation [1.4] solved for the electric field in the Z" direction.

$$E''_z = .053Z''_x + .0491X''_y \qquad [2.4]$$

Only the first term on the right of equation [2.4] is non-zero for this situation, the seismic mass can only produce shear in the Z_x direction. This transducer will operate in a shear mode and the output will be unaffected by off-axis acceleration.

CHAPTER III

TRANSDUCER DYNAMIC MODEL

The dynamic model for a piezoelectric transducer can be derived by writing a wave equation in terms of the electromechanical properties of the transducer and applying the appropriate boundary conditions. An alternative better suited to transducers with complicated electrode geometry, is the application of Green's functions at the electrode edges (3). Either method involves solution of equations in nine dimensions.

A transducer will have many resonant vibrational modes as standing waves are set up in each of the three principle directions. If we are concerned only with the potential developed across a pair of electrodes the exact three dimensional physical vibration of the piezoid does not need to be known. Rather, the operational characteristics of the transducer are of concern.

In the vicinity of a resonant frequency, the operational characteristics of the transducer can be modeled using a one-dimensional ordinary differential equation. The dynamic behavior of the transducer may be more familiarly modeled as a circuit having the same descriptive differential equation. The circuit used to model the transducer is shown in Figure 3. This model is valid near one resonant frequency of the transducer (3).

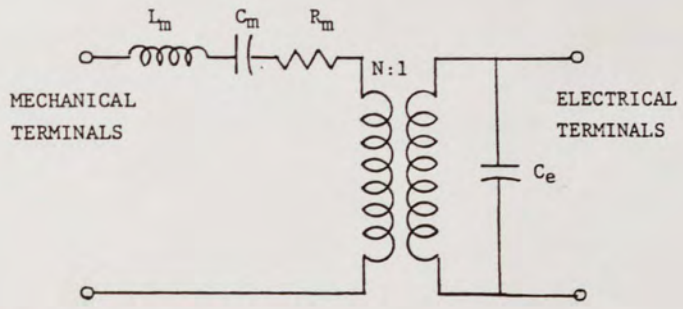

Figure 3. Model of a Piezoelectric Transducer Near One of its Resonant Vibrational Modes.

Force in the mechanical leg of the circuit is represented as input voltage. Current represents velocity and charge on C_m represents displacement or strain of the transducer. C_m represents the compliance or compressability of the transducer; mass or resistance to acceleration is modeled by L_m, and R_m accounts for losses in the transducer material itself and losses due to bonding. This model of the mechanical portion of the circuit is just that of a second order vibrating system (the lowest order model that can be used). Notice that if we leave the electrical terminals open and apply a mechanical force that the resulting voltage (and hence charge) on C_e is reduced due to potential developed across C_m. The open circuited transducer appears mechanically less compliant because compression induces electrical displacement, the induced electric field causes stress (by the inverse piezoelectric effect) which opposes the applied force and results in reduced overall

strain. The electromechanical turns ratio, N, models the efficiency of coupling of mechanical energy to electrical energy. It is a function of transducer physical properties and the mode of vibration being excited.

The values of all elements in the circuit may be determined in terms of the physical properties of the transducer and the transducer geometry. Solutions to equations for transducers involve mathematics in nine dimensions and are quite involved (3). Results of such calculations found in literature will not apply directly to these accelerometers due to the effect of the seismic mass and the bonding of the piezoelectric element to a base plate. For these reasons, the accelerometer will be characterized experimentally rather than with theoretical calculations.

We are concerned with the functional description of the transducer rather than in finding values of circuit model elements; we can reflect the mechanical portion of the circuit into the electrical leg. This will result in scaling of the elements in the mechanical leg of the circuit and the input force. The model to be used in analysis is shown in Figure 4; the electrical loading of the circuit due to the electrometer is indicated.

Solution of the circuit in the Laplace domain results in equation [3.1]. The input impedance of the electrometer was assumed to be purely resistive and in shunt to the amplifier.

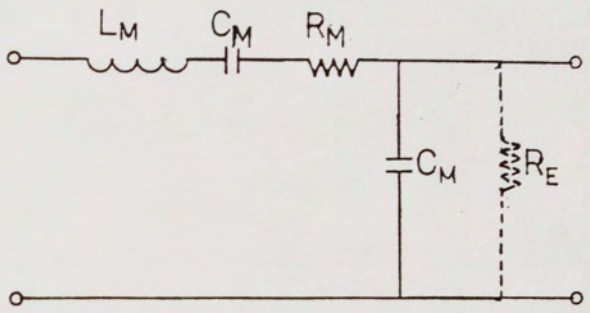

Figure 4. Transducer Model Used in Analysis.

$$\frac{A_0 S}{S^3 + A_1 S^2 + A_2 S + A_3} = \frac{V(s)}{|A(s)|}$$

$$A_0 = \frac{K}{L_m C_e} \qquad A_2 = \frac{1}{L_m C_e} + \frac{R_m}{L_m R_{in} C_e} + \frac{1}{L_m C_m}$$

$$A_1 = \frac{1}{L_m C_m R_{in} C_e} \qquad A_3 = \frac{1}{L_m C_m R_{in} C_e} \qquad [3.1]$$

Each accelerometer must now be characterized by determining the coefficients in equation [3.1].

CHAPTER IV

ELECTRICAL TESTING

The coefficients of equation [3.1] must be found to describe the behavior of a transducer. Methods currently used to characterize piezoelectric transducers involve testing both the electrical and mechanical behavior of the device.

Each of the methods requires the use of specialized test equipment that is uncommon in the electrical engineering laboratory. Furthermore, characterizations may be incorrect if reciprocity is blindly assumed. For example, suppose a piezoid is to be used as a sonar transducer. If characterization is accomplished by exciting the transducer electrically, and measuring the mechanical response, this characterization may not describe the behavior of the transducer when it is mechanically excited. Mechanical excitation can result in different transducer vibrational modes. Consequently, values of L_m, R_m, and C_m obtained from electrical excitation may not be valid when the transducer is subjected to mechanical excitation.

Due to anisotropy an electrical input may excite different modes of vibration, in certain transducers, than would a mechanical input of the same frequency. Even when mechanical and electrical inputs excite the same transducer vibrational mode, difficulty may exist. Mechanical and electrical inputs may excite vibrations of different relative amplitudes in each of the coordinate directions

in the piezoid, and thus the transducer will exhibit different dynamic properties. In other words, the transducer will vibrate differently for different forcing functions. A procedure will be outlined that will permit characterization of transducers by making only electrical test measurements. A method will be proposed and tested that will determine cases where electrical testing is invalid. The results of these tests will be compared with results of actual acceleration tests.

Let's turn our attention to the circuit model of Figure 4. For convenience, the impedance of the parallel electrical elements will be referred to as Z_e, and the impedance of the three mechanical elements will be called Z_m. If the transducer is driven by an electrical source, the mechanical terminals will appear as a short circuit as no external force will impede the strain of the transducer. The measured input impedance will then be

$$Z_{in} = \frac{Z_e Z_m}{Z_e + Z_m} \qquad [4.1]$$

Equation [4.1] can be algebraically manipulated to express mechanical impedance as a function of zero stress input impedance and impedance of the electrical leg.

$$Z_m = \frac{Z_{in} Z_e}{Z_e - Z_{in}} \qquad [4.2]$$

The mechanical impedance is that of a series resonant circuit as shown in Figure 4. The mechanical resistance is the minimum impedance which is found at the series resonant frequency. The mechanical inductance and capacitance can be found from knowledge of the antiresonant frequency and the slope of the attenuation at high frequencies. We first must determine the electrical impedance to allow us to solve for the mechanical properties. If the transducer is mechanically restrained (clamped), then electrical excitation will result in mechanical stress without any strain. The mechanical terminals will appear as an open circuit, and the electrical impedance can easily be measured. The electrical capacitance can easily be determined by knowledge of resistance and the pole frequency of the clamped transducer when subjected to sinusoidal electrical excitation. Then, this information along with the zero strain input impedance can be used in conjunction with equation [4.2] to find the mechanical element values. Finally, the transducer may be characterized by use of equation [3.1]. It should be noted that the transfer function can be found to within a constant. Because no input stress is used to test the transducer, the electromechanical turns ratio (N) of Figure 3 (which scales the acceleration input) cannot be determined.

The validity of the test method must be examined. As stated before, exact determination of the dynamic behavior of an anisotropic transducer requires solution of a nine-dimensional tensor wave equation. We will attempt to glean information pertaining to the dynamic behavior of the transducer based upon static equations for the transducer. The static equations will be used to examine how the transducer is driven or excited by various mechanical and electrical inputs.

Consider the ceramic transducer of Chapter 1. If stress is applied in the Z-direction, the resulting strain may be found by equation [1.2a]. Although this equation is for use in statics, it will give some insight into how the transducer will be excited by a time varying stress. We wish to characterize this response by performing a test. In the test we apply a time varying potential to electrodes on the positive and negative Z-faces. Equation [1.2b] gives insight into the type of vibration that will result. If this test is to be valid to characterize the response with a one-dimensional equation, the vibration of the transducer should be similar in both cases. The necessary condition for validity is that the transducer have the same vibrational mode for both electrical and mechanical excitation and that the vibration in each coordinate direction have the same relative amplitude.

If mechanical stress is applied in the Z-direction of a PZT-5 transducer, the resulting strain is found to be:

$$x_x = s_{13} Z_z$$

$$y_y = s_{13} Z_z$$

$$z_z = s_{33} Z_z \qquad [4.3]$$

If electric potential between z-electrodes is applied, the resulting strain is found to be:

$$x_x = d_{31} E_z$$

$$y_y = d_{31} E_z$$

$$z_z = d_{33} E_z \qquad [4.4]$$

Comparing equations [4.3] and [4.4], we see that the mode of vibration for each type of excitation will be the same. To roughly compare the relative vibrational amplitudes examine the following ratios.

$$\frac{d_{31}}{s_{13}} = 22.2$$

$$\frac{d_{33}}{s_{33}} = 19.9$$

Relative amplitudes are reasonably close (numerical values of electromechanical properties that are published for ceramics are representative averages (i.e., not exact) (2). Electrical testing of electromechanical properties of ceramics that are poled normal to their electrodes will yield acceptable results.

Similar calculations for a BT-cut quartz plate are very tedious, as double rotation is required to transform both the compliance and the piezoelectric stress coefficient matrices. The results are shown in Table 2, which lists the ratio of mechanically induced strain to electrically induced strain. Recall that the transducer measures shear stress Z_x and produces an electrical output E_z in the rotated coordinate system.

Poor results are expected from electrical testing of this transducer. Similar comparison of the X-cut quartz plate shows that stress along the X-axis will result in strain in the Z-direction while electric potential applied across the X-faces will not produce strain in this direction. (In general, electrical potential will never produce strain in quartz along the Z-axis. This axis in quartz is termed the optical axis; it exhibits no piezoelectric properties.) The electrical excitation results in a different mode of vibration than does mechanical excitation. For this reason, the X-cut quartz plate accelerometer is particularly unsuitable for characterization via electrical testing.

TABLE 2

RATIO OF MECHANICALLY INDUCED TO ELECTRICALLY INDUCED STRAIN FOR A BT-CUT QUARTZ PLATE

DIRECTION	RATIO
x_x	8.32
y_y	3.81
z_z	2.03
y_z	2.64
z_x	8.34
x_y	4.80

CHAPTER V

ELECTROMETER DESIGN

The function of the electrometer is to provide necessary amplification of the electric potential developed by the transducer without loading down the transducer. An electrometer must be utilized for acceleration testing to be accomplished. To uncover electrometer design considerations, we will investigate the response of the accelerometer to a step acceleration input. The major goal of this design is to extend the accelerometer response to as low a frequency as possible while concurrently maintaining simplicity. Low frequency response will depend upon electrometer input resistance. The design will utilize commercially available operational amplifiers as they are ideally suited for DC applications.

Consider the response of the model shown in Figure 4 to a step acceleration input. The transducer will experience strain; its rate of deformation will be controlled by the mass of the transducer and any friction present. Finally, the transducer will stop deforming (amount of strain depends on material stiffness). The charge accumulated on C_m represents this strain. The strain will result in dipole separation which can be measured as a potential difference across C_e.

Charge will leak through R_{in}; this charge will negate the potential due to dipole separation. As the electric potential across C_e drops toward zero, the transducer relaxes and undergoes further strain. This is represented in the model by C_m continuing to charge as the potential on C_e decays toward zero due to current flow through the electrometer.

It is evident that the low frequency response of the accelerometer is dependant upon the input resistance of the amplifier. The obvious solution seems to be to attach the transducer directly to the input of a MOS noninverting amplifier. These amplifiers have very high input impedance, which will permit operation to extremely low frequencies. Unfortunately, input bias currents (which may be modeled as current sources in series with the op amp input) (5) will integrate voltage across C_e and the amplifier will soon saturate. This situation is depicted in Figure 5.

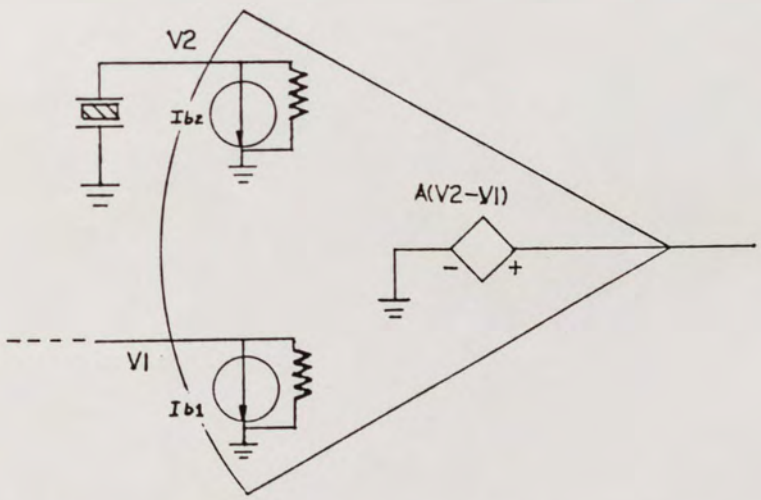

Figure 5. Op-amp Model used for Circuit Analysis.

A path must be provided for input bias current. A resistor can be placed in parallel with the transducer to accomplish this. Unfortunately, the input resistance of the amplifier will be severely reduced. The low frequency response of the accelerometer has been degraded. A component of sufficient resistance to give the desired time constant is not available. The input resistance can be increased by reducing the voltage drop across this parallel resistor. Figure 6 shows a bootstrap configuration. Positive feedback is used to reduce the voltage drop across R3 and increase amplifier input resistance. R1 and R2 are set up as a voltage divider from the op amp output. The positive feedback will place a voltage very close to the input resistance at the bottom of R3. Unfortunately, this creates a new problem. This positive feedback will cause the output due to input bias currents to be very high. Analysis shows that, for the worst case, the output can be several volts when the input terminal is left open (notice the transducer capacitance will make the input appear as an open to DC).

A multiplying resistor (R5) can be placed in series with the inverting input to negate the effects of input bias current. The circuit of Figure 6 was analyzed to allow minimization of output voltage due to offset current. The rather cumbersome result is

$$V_{out} = \frac{I_1\left(R5 + \frac{R4R6}{R4 + R6}\right) - I_2\left(R3 + \frac{R1R2}{R1 + R2}\right)}{\frac{R4}{R4 + R6} - \frac{R2}{R1 + R2}} \qquad [5.1]$$

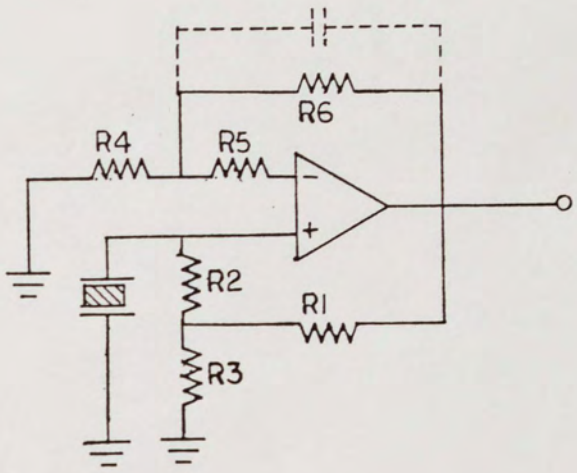

Figure 6. Amplifier Configuration.

To minimize the numerator we get the intuitive result that the impedance seen by each op amp input terminal must be equal.

$$\frac{R4R6}{R4 + R6} + R5 = \frac{R1R2}{R1 + R2} + R6 \qquad [5.2]$$

Satisfying equation [5.2] does not solve the problem entirely. Input offset current can still result in a significant output because of the large values of R1 and R5 needed. To reduce this we will try to maximize the denominator of equation [5.1].

$$|R1R4 - R2R6| = \text{maximum} \qquad [5.3]$$

It can be shown that the gain of this amplifier reduces to that of the standard noninverting op amp for very large open loop gain.

$$G_v = 1 + \frac{R6}{R4} \qquad [5.4]$$

The circuit of Figure 6 was analyzed to find the input impedance.

$$Z_{in} = \frac{R3}{\left[1 - \frac{R2(R1 + G_v R3)}{R1R2 + R1R3 + R2R3}\right]} \qquad [5.5]$$

Equations [5.2] through [5.5] form the set of design equations necessary to select the correct resistor values for the electrometer. Other topologies were studied, but none studied provided sufficient independence in adjusting D.C. gain, input resistance, and immunity to bias currents. The design selected also permits modification to implement a low pass filter to reduce noise without affecting input impedance or positive feedback (in the passband).

CHAPTER VI

MECHANICAL TESTING

To verify the electrical characterization of the accelerometer, the device will be subjected to a known acceleration while the output is recorded. The coefficients of equation [3.1] can then be found. The coefficients derived from the acceleration test will be compared with those found using the electrical test, as outlined in Chapter 4, to determine the validity of the electrical test.

To characterize a system, it is necessary to expose the system to inputs of all frequencies within the systems effective bandwidth. This can be accomplished by driving the system with an impulse. An impulse theoretically contains every frequency component. Practically speaking, for test purposes, the pulse must be of short enough duration so that its spectral content is constant over the bandwidth of the system being tested.

If the accelerometer is held stationary in the Earth's gravitational field, then placed in free-fall at time t = 0, and finally is arrested abruptly by colliding with a surface at t = T1, the acceleration profile that would be experienced is shown in Figure 7. The impulse imparted at collision would have area gT1 (Here it is assumed that air friction at low velocities will have negligible effect.)

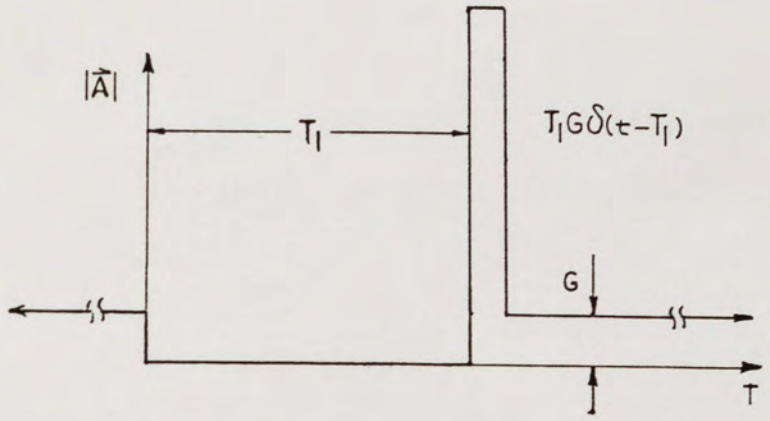

Figure 7. Acceleration Profile Used to Determine Accelerometer Impulse Response.

To use unilateral Laplace Transform theory, inputs must be zero before t = 0. The acceleration present for t < 0 can be replaced by a boundary condition. This can be incorporated into the forcing function by use of an initial condition generator (9). The initial condition generator will account for the initial charge on C_m at t = 0. The generator will produce a signal v(0)/s. For this case, v(0) = -kg. In the time domain 1/s corresponds to a unit step. Therefore, we can replace the initial condition with an additional input consisting of a step at t = 0 having magnitude -kg. This input is shown in equation [6.1].

$$A(t) = -kg\delta_1(t) + kgT_1\delta_0(t - T_1) + kg\delta_1(t - T_1) \qquad [6.1]$$

Now, working from the other side we start with equation [3.1]. A sampled data substitution is made for s. The bi-linear Z-transform is used. z^{-1} is interpreted as a delay operator that acts on v(t) and a(t). Equation [6.2] expresses the unknown coefficients of equation [3.1] in terms of the known acceleration and the system response to that acceleration.

$$6T^3A_3B_3 + T^2A_2B_2 + 6TA_1B_1 - T^2A_0B_0 = -12D \qquad [6.2]$$

$$D = V(nT) - 3V[(n-1)T] + 3V[(n-2)T] - V[(n-3)T]$$

$$B_0 = A(nT) + 9A[(n-1)T] - 9A[(n-2)T] - A[(n-3)T]$$

$$B_1 = V(nT) - V[(n-1)T] - V[(n-2)T] + V[(n-3)T]$$

$$B_2 = V(nT) + 9V[(n-1)T] - 9V[(n-2)T] + v[(n-3)T]$$

$$B_3 = V[(n-1)T] + V[(n-2)T]$$

To solve for the four unknowns in equation [6.2], four equations are needed. We can generate as many equations as we desire. One possible set is shown in equation [6.3].

$$\begin{pmatrix} -B_0(n) & B_1(n) & B_2(n) & B_3(n) \\ -B_0(n+1) & B_1(n+1) & B_2(n+1) & B_3(n+1) \\ -B_0(n+2) & B_1(n+2) & B_2(n+2) & B_3(n+2) \\ -B_0(n+3) & B_1(n+3) & B_2(n+3) & B_3(n+3) \end{pmatrix} \begin{pmatrix} A_0T^2 \\ 6A_1T \\ A_2T^2 \\ 6A_3T^3 \end{pmatrix} = 12 \begin{pmatrix} -D(n) \\ -D(n+1) \\ -D(n+2) \\ -D(n+3) \end{pmatrix} \quad [6.3]$$

Equation [6.3] can be solved for the coefficients of equation [3.1].

$$\underline{B} = \underline{AD}$$

$$\underline{A} = \underline{BD}^{-1} \quad [6.4]$$

Notice that the constants gk have been suppressed. Solution of equation [6.4] will yield the transform of the response of a transducer to a unit g acceleration. Equation [6.5] will be solved for several hundred sets of the coefficient $\underline{A}$, and the values will be averaged.

CHAPTER VII

RESULTS

During electrometer design the trade-offs between gain, input impedance, and output voltage due to offset current, became evident. These quantities are approximately related by the design equation:

$$V_{out} \sim Z_{in} G_v I_{os} \qquad [7.1]$$

where Z_{in} is given in equation [5.5]. To afford sufficient sensitivity during testing, the electrometer was constructed with $G_v = 40$. A potentiometer was used for R1 and the input resistance was adjusted to 500 MΩ. Low offset current JFET op-amps were used. Despite this, a D.C. output voltage of several tenths of a volt was observed. This output voltage changed with I_{os} (temperature). When the circuit was operating at high temperatures, the D.C. output was as high as two volts.

A high-pass filter can be used to remove the D.C. output voltage. The zero of the filter should be perhaps a decade lower in frequency than the minimum operating frequency of the accelerometer. If a filter is used, the D.C. output of the electrometer is of no consequence providing that the dynamic range of the accelerometer output voltage is not drastically reduced.

Four different accelerometers were constructed; two using BT-cut quartz and two using ceramic transducers. The input impedance of equation [4.1] could not be found directly. The network analyzers available could not make measurements down to the required low frequencies. A Hewlett-Packard 3582A spectrum analyzer was used to make measurements. Z_{in} can be found if two electrical ports are available to make measurements.

A resistor of known value was placed in series with the transducer. The ratio of input voltage (across resistor and transducer) to voltage drop across the transducer was measured with the spectrum analyzer. Measurements were made using two methods. In the first method, a white noise source was applied at the input and measurements made. In the second method, an oscillator was used and was swept through the frequencies of interest. Each method produced the same result. Next, a clamped measurement was made and C_e determined. Then Z_m was solved for. Once Z_m was known, estimations of C_m, L_m, and R_m were made at each frequency using equations [7.2a] through [7.2c].

$$R_m = Re(Z_m) \qquad [7.2a]$$

$$C_m = (f_1^2 - f_2^2)/2\pi f_1 f_2 (Z_{m1} f_2 - Z_{m2} f_1) \qquad [7.2b]$$

$$L_m = (Z_m + 1/2\pi f C_m) 1/2\pi f \qquad [7.2c]$$

The results were inconclusive. The standard deviation in values found for C_m, L_m, and R_m exceeded the mean by a factor of ten.

CHAPTER VIII

CONCLUSION

The inconclusive result was most likely caused by inadequate precision in the data sets that were taken. For small attenuation, the spectrum analyzer only provides one digit measurements. For larger attenuation, two significant digits are supplied. The effect of this was tested by computing Z_{in} for a theoretical circuit with known values of C_e, C_m, R_m, and L_m. Equations [4.2] and [7.2] were applied to solve for the circuit component values. The results were studied as the precision of the input data was varied.

Results were poorest for low Q circuits. (Note that the transducer has a very low Q. The bonding of the piezoid to its base results in a very large value of R_m. Inspection of the data which was gathered reveals no discernable resonant behavior).

Input data having six significant figures did not result in accurate prediction of circuit components over all frequency ranges. Capacitor values can only be found at lower frequencies. Inductor and resistor values were most accurately determined at intermediate frequencies where X_L and X_C are of comparable magnitude. (At higher frequencies, C_e shorts out the mechanical leg.)

As precision dropped below six digits, skill was required in interpreting the results of calculations: accurate results could

still be obtained. At 3 1/2 digits precision, calculations produced results which could not be correctly interpreted.

The electrical test procedure is theoretically valid. It is somewhat doubtful that electrical measurements can provide 3 1/2 digits of precision. A possible solution to the dilemma is to replace R_{in} with an inductor. This will force resonant responses from the transducer. This may permit characterization of low Q transducers. (On the down side, this will require analysis of a 4th order system.)

APPENDICES

APPENDIX A

PHYSICAL PROPERTIES OF SELECTED MATERIALS

The information regarding physical properties of quartz and PZT-5 was taken from reference (3). The general forms apply to all material having the same crystal structure. The form used for PZT-5 is applicable to all ferroelectric ceramics.

APPENDIX B

ROTATION MATRICES

The three-by-three rotation matrices were taken from reference (2). The-six-by six matrices were derived using concepts in reference (1). Stress vectors are transformed by pre-multiplication by a rotation matrix. Strain vectors are transformed by pre-multiplying by the conjugate transpose of the rotation matrix.

$$\underline{U} = \begin{pmatrix} c^2 & 0 & s^2 & 0 & -2sc & 0 \\ 0 & 1 & 0 & 0 & 0 & 0 \\ s^2 & 0 & c^2 & 0 & 2sc & 0 \\ 0 & 0 & 0 & c & 0 & s \\ sc & 0 & -sc & 0 & c^2-s^2 & 0 \\ 0 & 0 & 0 & -s & 0 & c \end{pmatrix}$$

$$\underline{u} = \begin{pmatrix} c & 0 & -s \\ 0 & 1 & 0 \\ s & 0 & c \end{pmatrix}$$

$c = \cos(q)$

$s = \sin(q)$

$$\underline{V} = \begin{pmatrix} c^2 & s^2 & 0 & 0 & 0 & 2sc \\ s^2 & c^2 & 0 & 0 & 0 & -2sc \\ 0 & 0 & 1 & 0 & 0 & 0 \\ 0 & 0 & 0 & c & -s & 0 \\ 0 & 0 & 0 & s & c & 0 \\ -sc & sc & 0 & 0 & 0 & c^2-s^2 \end{pmatrix}$$

$$\underline{v} = \begin{pmatrix} c & s & 0 \\ -s & c & 0 \\ 0 & 0 & 1 \end{pmatrix}$$

$c = \cos(r)$

$s = \sin(r)$

$$\underline{T} = \begin{pmatrix} 1 & 0 & 0 & 0 & 0 & 0 \\ 0 & c^2 & s^2 & 2sc & 0 & 0 \\ 0 & s^2 & c^2 & -2sc & 0 & 0 \\ 0 & -sc & sc & c^2-s^2 & 0 & 0 \\ 0 & 0 & 0 & 0 & c & -s \\ 0 & 0 & 0 & 0 & s & c \end{pmatrix}$$

$$\underline{t} = \begin{pmatrix} 1 & 0 & 0 \\ 0 & c & s \\ 0 & -s & c \end{pmatrix}$$

$c = \cos(p)$

$s = \sin(p)$

Coefficient Matrices for PZT-5

$$\underline{K} = \begin{pmatrix} K_{11} & 0 & 0 \\ 0 & K_{11} & 0 \\ 0 & 0 & K_{33} \end{pmatrix}$$

$$\underline{d} = \begin{pmatrix} 0 & 0 & 0 & 0 & d_{15} & 0 \\ 0 & 0 & 0 & d_{15} & 0 & 0 \\ d_{31} & d_{31} & d_{33} & 0 & 0 & 0 \end{pmatrix}$$

$$\underline{s} = \begin{pmatrix} s_{11} & s_{12} & s_{13} & 0 & 0 & 0 \\ s_{12} & s_{11} & s_{13} & 0 & 0 & 0 \\ s_{13} & s_{13} & s_{33} & 0 & 0 & 0 \\ 0 & 0 & 0 & s_{44} & 0 & 0 \\ 0 & 0 & 0 & 0 & s_{44} & 0 \\ 0 & 0 & 0 & 0 & 0 & (s_{11}-s_{12}) \end{pmatrix}$$

Coefficient Matrices for Quartz

$$\underline{k} = \begin{pmatrix} k_{11} & 0 & 0 \\ 0 & k_{11} & 0 \\ 0 & 0 & k_{33} \end{pmatrix}$$

$$\underline{d} = \begin{pmatrix} d_{11} & -d_{11} & 0 & d_{14} & 0 & 0 \\ 0 & 0 & 0 & 0 & -d_{14} & -2d_{11} \\ 0 & 0 & 0 & 0 & 0 & 0 \end{pmatrix}$$

$$\underline{s} = \begin{pmatrix} s_{11} & s_{12} & s_{13} & s_{14} & 0 & 0 \\ s_{12} & s_{11} & s_{13} & -s_{14} & 0 & 0 \\ s_{13} & s_{13} & s_{33} & 0 & 0 & 0 \\ s_{14} & -s_{14} & 0 & s_{44} & 0 & 0 \\ 0 & 0 & 0 & 0 & s_{44} & s_{14} \\ 0 & 0 & 0 & 0 & s_{14} & 2(s_{11}-s_{12}) \end{pmatrix}$$

TABLE 3

ELECTROELASTIC COEFFICIENTS FOR QUARTZ
(MKS UNITS)

$s_{11} = 12.77 \times 10^{-12}$	$d_{11} = 2.31 \times 10^{-12}$
$s_{33} = 9.60 \times 10^{-12}$	$d_{14} = 0.727 \times 10^{-12}$
$s_{12} = -1.79 \times 10^{-12}$	$k_{11} = 4.52\ \varepsilon_o$
$s_{13} = -1.22 \times 10^{-12}$	$k_{33} = 4.68\ \varepsilon_o$
$s_{44} = 20.04 \times 10^{-12}$	
$s_{66} = 29.12 \times 10^{-12}$	
$s_{14} = 4.50 \times 10^{-12}$	

TABLE 4

ELECTROELASTIC COEFFICIENTS FOR THE
LEAD-ZIRCONATE-TITANATE CERAMIC PZT-5
(MKS UNITS)

$s_{11} = 16.4 \times 10^{-12}$	$d_{31} = -171 \times 10^{-12}$
$s_{33} = 18.8 \times 10^{-12}$	$d_{33} = 374 \times 10^{-12}$
$s_{12} = -5.74 \times 10^{-12}$	$d_{15} = 584 \times 10^{-12}$
$s_{13} = -7.72 \times 10^{-12}$	$k_{11} = 1730\ \varepsilon_o$
$s_{44} = 47.5 \times 10^{-12}$	$k_{33} = 1700\ \varepsilon_o$
$s_{66} = 44.3 \times 10^{-12}$	

REFERENCES

1. Crandall, S.H.; Dahl, N.C.; and Lardner, T.J. An Introduction to the Mechanics of Solids, 2nd Ed. New York: McGraw-Hill, 1978.

2. Buchanan, R.C., et al. Ceramic Materials for Electronics. New York: Marcel-Dekker, Inc., 1986.

3. Holland, R., and EerNisse, E.P. Design of Resonant Piezoelectric Devices. Cambridge, MA: M.I.T. Press, Research Monograph No. 56, 1969.

4. Bottom, V. Introduction to Quartz Crystal Unit Design. New York: Van Nostrand-Reinhold, 1982.

5. Wait, J.; Huelsman, L.P.; and Korn, G.A. Introduction to Operational Amplifier Theory and Applications. New York: McGraw-Hill, 1975.

6. Martin, R.J. "Analysis and Synthesis of Active Feedback Applied to Piezoelectric Devices." Ph.D. dissertation, University of Central Florida, 1984.

7. Barrow, W.H. "Testing of Active Feedback Applied to Piezoelectric Devices." Master's research report, University of Central Florida, 1983.

8. Parzen, B. Design of Crystal and Other Harmonic Oscillators. New York: John Wiley and Sons, 1983.

9. Hayt, W.H., Jr., and Kemmerly, J.E. Engineering Circuit Analysis. New York: McGraw-Hill, 1978.

10. Motamedi, M.E. "Acoustic Accelerometers." IEEE Transactions on Ultrasonics, Ferroelectrics, and Frequency Control 34 (March 1987): 237-242.